Role of intra-adsorbate Coulomb correlations in energy transfer at metal surfaces

M. Plihal and David C. Langreth

Department of Physics and Astronomy, Rutgers University, Piscataway, New Jersey 08854-8019

(Received 20 November 1997)

We present and discuss a theory of electronic friction for open-shell atomic or molecular adsorbates moving normal to a metallic surface. The theory applies to the case where the intra-adsorbate Coulomb interaction splits the positive- and negative-ion peaks in the spectral density of the adsorbate by an amount larger than their widths, and where one of them is much nearer the Fermi level than the other. We distinguish two limits: (i) the low-temperature friction regime where the friction is caused by the overlap of the adsorbate level's width and the Fermi level, and (ii) the high-temperature friction regime, where the friction is caused by thermally induced transitions. In regime (i) we find a large *enhancement* in the friction in many cases due to the Kondo effect, which can occur even at very high temperatures. In this region, the frictional force is highly temperature and velocity dependent. In region (ii), on the other hand, we typically find a *reduction* in the friction, sometimes substantial, from what is found in the traditional theory. Our results should be applicable to the description of desorption induced by hot electrons, which has been called DIMET when in region (ii). [S0163-1829(98)01719-6]

I. INTRODUCTION

The energy transfer between atoms or molecules and surfaces plays an important role in dynamic processes such as adsorption and desorption, diffusion, and chemical reactions at surfaces. For many years, the dominant contribution to the energy transfer has been attributed to phonons. However, for a metallic surface, an additional mechanism exists in the form of coupling of the adsorbate degrees of freedom to the electron-hole pair excitations in the metal, as pointed out in pioneering theoretical work[1-8] starting two decades ago. In recent years, growing experimental evidence suggests that the electronic mechanism is important in a variety of surface phenomena.

The electron-hole mechanism has been suggested by Persson and Persson[9] as a determining factor in vibrational lifetimes of CO adsorbed on Cu(100). Infrared reflection spectroscopic studies of the system indeed show very little temperature dependence of the linewidths and thus suggest strong electronic involvement,[10,11] and line-shape studies confirm this view.[12,13] In addition, finite cluster modeling of the C-O stretch mode lifetimes[14] found the electronic mechanism sufficient to explain the experimentally observed broadening. Molecular-dynamics simulations with electronic friction included[15] compared the phonon and electronic contributions to vibrational lifetimes and found the electronic friction to dominate over the phonon damping for almost all vibrational modes of CO/Cu(100).

One of the challenges in experimental surface science has been the development of techniques that would allow us to study the microscopic nature of energy transfer and thus separate its contributions. In practice, this amounts to developing time-resolved experiments with resolution on time scales short compared with the typical rate of energy flow between the individual degrees of freedom. Recent advances made such an analysis possible in studies of desorption induced by ultrashort, subpicosecond laser pulses[16] carried out on CO/Cu(111) and NO/Pd(111) complexes. The laser light

is known to be absorbed by the substrate, rather than directly energizing the adsorbate. The system is characterized by highly nonequilibrium conditions over the duration of the laser pulse. The substrate electrons reach temperatures of about $T \sim 3000$ K and come to equilibrium with the lattice in approximately 1 ps. Since the specific heat of the lattice is much larger, the peak temperature in the lattice reaches only $T \sim 600$ K. The desorption time was found by double-pulsed experiments to be less than 1 ps, too short to be explained by the conventional thermal desorption, as the lattice temperatures would be too low to explain the high desorption rates. These results strongly indicate an electronic involvement. The mechanism of desorption induced by multiple electronic transitions (DIMET) has been proposed[17] and studied in detail[18] and shown to give semiquantitative agreement with the experiment data.

A more recent and quite spectacular manifestation of the importance of nonadiabatic electron processes on bond breaking appeared in connection with manipulating single atoms and molecules at surfaces via scanning tunneling microscopy (STM). In a landmark experiment,[19] Eigler, Lutz, and Rudge transferred, in a controlled and reversible way, a single Xe atom between nickel substrate and the STM tip. In a similar experiment, Stipe *et al.*[20] demonstrated dissociation of the molecule O_2 on Pt(111) surface at low temperatures with the STM tip. In both cases, the current of tunneling electrons excites the adsorbate from the bottom of the adsorption well in a stepwise manner, until it overcomes the adsorption barrier and hops to the neighboring potential well. This mechanism has been termed vibrational heating and is quite similar to the DIMET. It can be described in terms of competition between energy gain from the inelastically scattered tunneling electrons and simultaneous energy loss to electron-hole and phonon excitations in the metal.[21]

The important ingredient, common to the theories of the processes mentioned in the previous paragraphs, is the notion that a single, adsorbate induced resonance near the Fermi level dominates the energy transfer. The existence of such a

level is expected to be a rather general phenomenon. The response of metal electrons to the localized dynamic perturbation is known to violate the adiabatic theorem,[22] due to the localized nature of the perturbation and due to the availability of large number of low-energy excitations in the metal. It is this nonadiabatic coupling of electronic states to adsorbate degrees of freedom that drives the electronic processes considered here. Ultimately, the energy is dissipated through large number of low-energy electron-hole pair excitations in the metal.

All the theories reviewed here ignore the intra-adsorbate Coulomb interaction, which is known to produce, under certain circumstances, the Kondo and mixed valent correlated states, despite early work[5] suggesting the importance of such states. They appear in the local density of states as narrow resonances at the Fermi level. If the parameters are such that these states are formed, long electronic time scales are introduced and an additional source of nonadiabaticity is present. It is the purpose of this paper to make a systematic study of the effects of the correlated states and other many-body corrections on energy transfer. In our numerical calculations, we study specific models of adsorbate-metal complexes, but the general conclusions of this paper are independent of these choices. In addition, we show that intra-adsorbate Coulomb correlations can have a substantial effect on the electronic friction, even when one is in a parameter region where the Kondo-like states cannot form, such as in the thermally induced DIMET regime.

The structure of the paper is as follows. In Sec. II, we discuss the theoretical framework and approximations involved. Relevant details and derivations are arranged into appendices. In Sec. III, we discuss the numerical results, and we summarize our findings in Sec. IV.

II. CONCEPTUAL FOUNDATION AND THEORETICAL MODEL

We wish to describe the situation that is approximately described by the adsorbate moving along a diabatic potential-energy curve $V_0(R)$ outside a metal, as illustrated in Fig. 1. The electronic structure of the adsorbate is assumed to be dominated by the effect of a single degenerate energy level in the vicinity of the substrate's Fermi level. The occupation of this level is subject to change due to tunneling to and from the substrate, which give it a width Γ, and due to thermal fluctuations. When the adsorbate is in a negative (positive) ion excited state, its motion is controlled by the curve marked $V_1(R)$. This differs from $V_0(R)$ by the image potential (plus a constant) except at short distances.[23] Note that to the extent that Γ is not vanishing, each of these curves is a shorthand for a continuum of essentially parallel potential-energy curves, differing by the energies of the continuum of electron-hole excitations that are possible in the substrate. For most of this paper we suppose that the velocity of the adsorbate is sufficiently slow, that one is to average over the effect of multiple electronic transitions. In that case, the adsorbate will be driven by an average force derived from an average (adiabatic) potential curve $V(R)$ part way between the two curves shown, but typically much closer to $V_0(R)$. In addition, the fluctuations in the force on the particle lead to a dissipative or frictional force proportional to
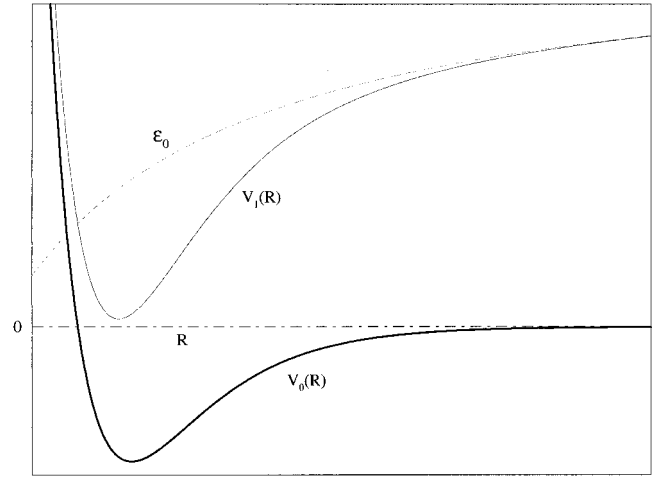

FIG. 1. Schematic diabatic potential energy curves for a neutral adsorbate V_0 and for negative (positive) ion state V_1. The difference between them (dashed line) is the energy ϵ_0 to excite the adsorbate to the negative (positive) ion state by transferring an electron (hole) from the substrate to the adsorbate.

the adsorbate's velocity at low velocities. At higher velocities, there are deviations from this picture that we also calculate.

A. Electronic friction and the Markovian limit of energy transfer

One standard way of describing the above situation, is to replace the equations describing the details of the motion and transitions of the individual electrons, and incorporate their effect in a single stochastic equation for the motion of the adsorbate, that is a generalized Langevin equation

$$M\ddot{R}(t) \equiv -\frac{1}{v(t)}\dot{E}(t) = -\frac{dV(R)}{dR} - \int_{-\infty}^{t} dt' \Lambda(t-t')v(t')$$
$$+ f(t). \tag{2.1}$$

More generally, one could take account of multiple dimensional adsorbate motions, as well as substrate atom motions through a set of coupled equations of this type,[24] but that would distract from the issues we wish to address here. Here, $v(t) = \dot{R}(t)$ is the velocity of adsorbate, $f(t)$ is a random force, and the integral proportional to $v(t)$ is the frictional force. The nonlocal kernel, $\Lambda(t-t')$, contains the dissipative forces and takes into account the dependence on the memory of the system. The contribution to $\Lambda(t-t')$ of the electronic degrees of freedom can be expressed in terms of the nonadiabatic coupling between electronic states. Frictional and random forces related by the fluctuation-dissipation theorem, which is an expression of the mechanism that drives the system toward local thermal equilibrium. One should not be misled by the simplicity of Eq. (2.1): for a nonuniform system the quantity Λ is a functional of $[R(t)]$; the more trivial dependence on $t-t'$, explicitly shown, is to facilitate the later discussion of the range of the nonlocality in time. The random force $f(t)$ has an autocorrelation function that is also a functional of $[R(t)]$.

The theory presented in this paper focuses on the dissipative forces of the Langevin equation in a regime where intra-adsorbate electron correlations are important. Specifically it is a theory of the frictional force integral,

$$\dot{E}_{\mathrm{non}}(t) = v(t) \int_{-\infty}^{t} dt' \Lambda(t-t') v(t'), \qquad (2.2)$$

in Eq. (2.1) for a specified $R(t)$ and not a theory of the full solution of Eq. (2.1) in an arbitrary force field.

There is one situation in which Eq. (2.2) becomes fairly simple, and that is where the adsorbate moves only a short distance during the time range of the kernel Λ. This could occur because of the constraints from the potential (e.g., a harmonic oscillation in the bottom of the well). But it always occurs for sufficiently small velocity v. In either of these cases one may use linear response theory in the displacement $R(t) - R(t')$ about the position $R(t')$ to calculate the frictional force at time t. The result is a force-force correlation function, which has been discovered and rediscovered by a number of groups.[2,25] This is particularly simple in the latter case, where the friction kernel in Eq. (2.2) becomes local:

$$\Lambda(t-t') = \delta(t-t') M \eta(R(t)), \qquad (2.3)$$

and the system dynamics is described by the standard Langevin equation,

$$M\ddot{R}(t) = -\frac{dV(R)}{dR} - M \eta(R(t)) v(t) + f(t). \qquad (2.4)$$

More generally, Eq. (2.4) is an approximation that we refer to as the local friction approximation (LFA). It becomes exact in the limit of small v. Its essential feature is that the dissipative force is describable by a simple friction coefficient η, whose only time dependence is through its position dependence $R(t)$. This paper focuses on determining the behavior of η in situations where Eq. (2.4) is valid, and more generally of Eq. (2.2), when it is not.

B. Hamiltonian

We describe the interaction between conduction electrons in the metal and the electrons on the localized adsorbate level by means of the time-dependent Anderson Hamiltonian,

$$H(t) = \sum_a \epsilon_{\mathrm{empty}}(t) n_a + \sum_{ak} \epsilon_k n_{ka} + \sum_{ak} [V_k(t) c_{ka}^\dagger c_a + \mathrm{H.c.}]$$

$$+ \sum_{a>a'} U(t) n_a n_{a'}. \qquad (2.5)$$

Here $\epsilon_{\mathrm{empty}}(t)$ is the instantaneous energy required to add the first electron to a previously empty adsorbate orbital complex. The index a enumerates the N relevant adsorbate orbitals, assumed degenerate. We assume that it corresponds to symmetries that are shared with the conduction electrons (including at least the conservation of a spin component, and possibly orbital symmetries such as the reflection through planes perpendicular to the surface as well), so that a can be used as a quantum number for the substrate electrons as well. Therefore the substrate band energy ϵ_k is assumed to depend
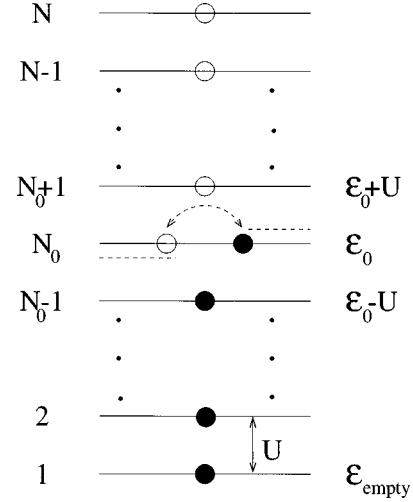

FIG. 2. Schematic representation of the single-particle energy levels in $V_{ka}=0$ limit of an N-fold degenerate adsorbate complex. N_0 labels the energy level ϵ_0 near the Fermi energy (dashed lines).

on the other quantum number k only. The quantity $n_{ka} = c_{ka}^\dagger c_{ka}$ is the number operator for the conduction electrons in the indicated state. The time-dependent hybridization matrix element between the substrate and adsorbate electrons is $V_k(t)$. The time dependence of the ϵ, V_k, and U parameters arises only by virtue of the fact that they are functions of spatial coordinate R, which in turn is time dependent.

Our basic model consists in assuming that U is large enough so that none of the other ionization states are relevant. This will be the case if $|\epsilon_0 \pm U - \epsilon_F| \gg \max(T,\Gamma)$ where $\epsilon_0 = \epsilon_{\mathrm{empty}} + (N_0-1)U$, Γ is the width of the level, and T is the temperature in energy units. It will not matter that U splits all ionization states equally or even that some may be unbound and in the continuum, because we really only use U as a device to exclude the ionization states that are far from the Fermi level and deemed to be irrelevant to the physics at hand. The spectrum of these states for the trivially soluble case $V_k=0$ is shown in Fig. 2; the levels refer to the energies required to add additional electrons, not total energies. This figure shows notation that we use throughout this paper. There are N ionization levels corresponding to the N-fold degeneracy of the orbitals, while the Fermi level of the substrate, indicated (for two possibilities) by the two dashed lines, lies near the ionization state containing N_0 electrons, so that this one can be either filled or empty. We can then effectively replace Eq. (2.5) by

$$H(t) = \sum_a \epsilon_0(t) n_a + \sum_{ak} \epsilon_k n_{ka} + \sum_{ak} [V_k(t) c_{ka}^\dagger c_a + \mathrm{H.c.}]$$
$$\qquad (2.6)$$

with the constraint that the subspace $|S\rangle$ within which $H(t)$ acts is just a subset of the original Fock space given by

$$\{|S\rangle; n=0,1\}, \qquad (2.7)$$

where

$$n = \sum_{a=1}^{N} n_a - N_0 + 1. \qquad (2.8)$$

It is the effect of the constraint (2.7) arising from the intra-adsorbate Coulomb correlations that is the topic of this work. We will refer to this as the $U=\infty$ case for a particular value of N, in contrast to the often used[18] $U=0$ model, consisting of the Hamiltonian (2.6) without the constraint (2.7). Of course, the two models coincide for the (essentially physically nonexistent) case of $N=1$. The intermediate region of finite U's effects our theory in two ways. (1) If the Coulomb repulsion does not separate the two levels sufficiently, so that the condition of the previous paragraph is violated, our theory breaks down qualitatively. (2) The quantitative conclusions of our theory become inaccurate, e.g., estimates of Kondo temperature, unless $U \gg |\epsilon_0|$. One further remark: There is no necessity that the creation operators in Eqs. (2.5) and (2.6) be defined to create particles—they could just as well have been defined to create holes instead; this means that at the present level, the case $N_0=1$ is the same as $N_0=N$, $N_0=2$ is the same as $N_0=N-1$, and so on.

We give some practical examples. (i) CO standing upright over a Cu surface: fourfold degenerate π^* affinity level a little above the Fermi level, so that $N=4$, $N_0=1$, essentially a closed-shell case, where no major correlation effects are expected. (ii) A Li atom moving 8 a.u. outside of an Al surface (or closer to a cesiated one): ionization level a little below Fermi level, affinity level several eV higher, or essentially out of the picture, so that $N=2$, $N_0=1$; major differences between $U=0$ and $U=\infty$. (iii) NO upright over Cu surface with temperature much larger than the spin-orbit splitting: positive ion state several eV below the Fermi level, and out of the picture; the negative ion state an eV or so above Fermi level is the active level, so that $N=4$, $N_0=2$; major differences from $U=0$ theory expected. (iv) NO oblique or lying over Cu: one π spatial orbital has larger Γ than the other, so that the effect of the weakly coupled one can be neglected; $N=2$, $N_0=2$ (or $N=2$, $N_0=1$ in the equivalent description in terms of holes); major differences from the $U=0$ theory expected.

The complete model Hamiltonian that would yield the generalized Langevin equation (2.4) would in addition to the Hamiltonian (2.6) contain the kinetic energy of the adsorbate $\frac{1}{2}M\dot{R}^2$ and the diabatic potential $V_0(R)$. The multiple transitions between the curves V_0 and V_1 in Fig. 1 are described by the first term in Eq. (2.6): ϵ_0 depends on t through its dependence on $R(t)$, and $V_1(R)-V_0(R)=\epsilon_0(R)$. From now on, we will imagine that R is simply the one-dimensional distance z from the surface.

We conclude this section by discussing the parameterizations of the quantities in the Hamiltonian (2.6) that we follow here. We define the full width parameter Γ as

$$\Gamma(\epsilon,t) = 2\pi \sum_k |V_k(t)|^2 \delta(\epsilon-\epsilon_k), \qquad (2.9)$$

which is, to lowest order, the adiabatic tunneling rate between the band and the adsorbate level electrons. We assume that the k dependence of $V_k(t)$ comes only in the form of ϵ_k and that its shape is time invariant. In this case, the potential is separable $V_k(t) \equiv u(t)v(\epsilon_k)$. Note that by doing this we are excluding the effects of the variations in the *phase* of $V_k(t)$. In the one-dimensional case treated here, this does not matter, but for motions parallel to the surface, variations in

the phase are what give the friction entirely, so that the theory presented here is incomplete. The effects arising from these phase variations for parallel motion, or for some rotational motions, are very interesting, and will be the subject of a future paper. Using the above parametrization, the adiabatic tunneling rate $\Gamma(\epsilon,t)$ can be written

$$\Gamma(\epsilon,t) = 2\pi |u(t)|^2 \xi(\epsilon), \qquad (2.10)$$

where $\xi(\epsilon) = \rho(\epsilon)|v(\epsilon)|^2$ and $\rho(\epsilon)$ is the density of states. Here we take $\xi(\epsilon) = \frac{3}{2}[1-(\epsilon^2/D^2)]$ for $|\epsilon| \leq D$ and $\xi(\epsilon) = 0$ otherwise, with $D=5$ eV. All energies in this paper are measured from the Fermi level ($\epsilon_F = 0$). Note that Γ depends on both ϵ and t. If the value of ϵ is unspecified, it will refer to the value at $\epsilon = \epsilon_0(t)$, which most closely represents the actual width of the level. On the other hand, we will define the Fermi-level half-width parameter Δ, such that $\Delta(t) = \frac{1}{2}\Gamma(0,t)$.

C. Energy transfer

The rate of adding energy to a system described by Eq. (2.6), with or without the constraint, (see Appendix B for details) is

$$\dot{E}(t) = \sum_a \dot{\epsilon}_0(t)n_a(t) + \sum_{ka} [\dot{V}_k^*(t)n_{ak}(t) + \text{H.c.}], \qquad (2.11)$$

where $n_a(t) = \langle c_a^\dagger(t)c_a(t) \rangle$ and $n_{ak}(t) = \langle c_a^\dagger(t)c_{ka}(t) \rangle$, each independent of a in our case. The diagonal and off-diagonal occupation numbers $n_a(t)$ and $n_{ak}(t)$ do not follow their equilibrium values except in the very slow limit, and we denote the deviations from these values by $\delta n_a(t)$ and $\delta n_{ak}(t)$. The *nonadiabatic* energy transfer, as expressed by Eq. (2.2) is then given by

$$\dot{E}_{\text{non}}(t) = \sum_a \dot{\epsilon}_0(t)\delta n_a(t) + \sum_{ka} [\dot{V}_k^*(t)\delta n_{ak}(t) + \text{H.c.}]. \qquad (2.12)$$

Equation (2.12) can also be cast in a form, which is physically more intuitive and suitable for analytic approximations of certain limiting behavior. For that purpose, we introduce the Wigner distribution functions,

$$n_a(\omega,t) \equiv \int_{-\infty}^\infty d\tau \left\langle c_a^\dagger\left(t+\frac{\tau}{2}\right)c_a\left(t-\frac{\tau}{2}\right)\right\rangle e^{i\omega\tau}, \qquad (2.13)$$

with a corresponding expression for $n_{ak}(\omega,t)$. The off-diagonal function in Eq. (2.12) can be eliminated with the help of the Fourier transform of the equation of motion,

$$[\omega - \epsilon_0(t)]n_a(\omega,t) = \sum_k V_k^*(t)n_{ka}(\omega,t). \qquad (2.14)$$

Using Eq. (2.14), the equation for energy transfer can be written as

$$\dot{E}_{\text{non}}(t) = \int_{-\infty}^\infty \frac{d\omega}{2\pi}\left[\dot{\epsilon}_0(t) + \frac{\dot{\Delta}(t)}{\Delta(t)}[\omega - \epsilon_0(t)]\right]\delta n(\omega,t), \qquad (2.15)$$

where $\delta n(\omega, t) = \Sigma_a \delta n_a(\omega, t) = N \delta n_a(\omega, t)$. This provides an explicit expression suitable for numerical evaluation.

In the LFA limit, we can expand the expression (2.12) in powers of velocity v and keep the lowest term. This is readily done by expanding the function $\delta n(\omega, t)$ in Eq. (2.15). For the $U = 0$ case the result can be expressed in terms of the adiabatic phase shift for the Anderson model

$$\lim_{v \to 0} \dot{E}_{\text{non}}(t) \equiv M v^2 \eta(t) = N \int_{-\infty}^{\infty} \frac{d\omega}{\pi} \left(-\frac{\partial f(\omega)}{\partial \omega} \right) \dot{\delta}^2(\omega, t). \tag{2.16}$$

This result has been obtained by a number of authors.[18,5,4] For our case of a parabolic $\xi(\epsilon)$, the phase shift is given by

$$\tan \delta(\omega, t) = \frac{\xi(\omega) \Delta(t)}{\omega - \epsilon_0(t) - \dfrac{\lambda(\omega)}{\pi} \Delta(t)}. \tag{2.17}$$

Here, $\xi(\omega)$ is defined below Eq. (2.10), and

$$\lambda(\omega) \equiv P \int d\Omega \frac{\xi(\Omega)}{\omega - \Omega} = 3 \frac{\omega}{D} + \xi(\omega) \ln \frac{D + \omega}{D - \omega}.$$

Equation (2.16) [but not, of course, Eq. (2.17)] has been shown[5] to be valid for the interacting Anderson model in the very low temperature regime, as well.

One can use Eq. (2.17) to get a reference point for our discussion of correlation effects in the next two sections. Clearly, the friction will be large when ϵ_0 passes through the Fermi level, especially at low temperatures and for small width Δ. However, situations where ϵ_0 is near ϵ_F, but does not cross the Fermi level, are of great experimental interests. Then there are two ways in which the parameters can be such as to give a substantial contribution to Eq. (2.16): (i) the temperature is high enough to give the Fermi-function derivative in Eq. (2.16) sufficient width that the denominator in Eq. (2.17) can be small, and (ii) the half-width Δ is large enough that the numerator is large. These two cases have been clearly elucidated by Brandbyge et al.[18] In the first case the friction is caused by multiple thermally induced transitions between the curves in Fig. 1, a process that has been called DIMET (Ref. 17) when used to describe desorption induced by hot electrons. The other limit (ii) involves multiple transitions induced by the level width of the states, and is the more traditional friction mechanism invoked, for example, by Persson and Persson[9] or by Head-Gordon and Tully.[25] In Sec. II D below, we discuss the effects of the constraint (2.7) on the friction in the limit (i). Following that in Sec. II E we lay the groundwork for our discussion of the limit (ii), and also for our more general theory that bridges between the two limits. Our conclusion is that the effect of the constraint is significant, irrespective of where one is with respect to the above limiting cases in open-shell systems.

D. Electron friction induced by the temperature and the role of semiclassical master equations

An important limiting case of the theory, which can be called the semiclassical approximation (SCA), appears at high temperatures and for slowly moving adsorbates with narrow resonances satisfying the condition $|\epsilon_0 - \epsilon_F| \gg \Gamma$. The

exact criteria for validity of the approximation have been formulated by Shao et al.,[26] for the case $N_0 = 1$. This is the temperature-induced friction or DIMET limit of the theory. It is more important than this validity criteria would suggest, because at least one of the analytic results valid in this region persists in the other regions we have studied.

For small Γ the transitions may be described by Fermi golden rule master equations. For example, the rate of change of adsorbate occupation due to electrons tunneling *out* of the adsorbate can be written

$$\left(\frac{dn}{dt} \right)_{\text{out}} = -2\pi \sum_{fi} |\langle f| \sum_{ka} V_k c_{ka}^{\dagger} c_a |i\rangle|^2 \delta(E_f - E_i) P_i. \tag{2.18}$$

Here n, as defined by Eq. (2.8), is now an expectation value. The initial state $|i\rangle$ is the product of one of the N_0 particle adsorbate states of degeneracy $g = \binom{N}{N_0}$ and an arbitrary substrate state. The probability P_i is the product of occupation probability of this adsorbate state ($= n/g$) and the thermal occupation probability of the substrate state indicated by i. Straightforward evaluation yields

$$\left(\frac{dn}{dt} \right)_{\text{out}} = -\Gamma N_0 (1 - f_0) n, \tag{2.19}$$

where f_0 is the equilibrium Fermi function $(e^{\beta \epsilon} + 1)^{-1}$ at the energy $\epsilon = \epsilon_0(t)$ and $\Gamma = \Gamma(\epsilon_0(t), t)$. In a similar manner one can obtain the rate at which electrons enter the adsorbate, which when combined with Eq. (2.19), gives the master equation

$$\frac{dn}{dt} = -\Gamma[N_0(1 - f_0)n - (N - N_0 + 1)(1 - n)f_0]. \tag{2.20}$$

For $N_0 = 1$, this equation has been shown[27] to be the rigorous semiclassical limit of the more general equations discussed later in this paper. It should be contrasted with the master equation for the $U = 0$ case,

$$\frac{dn_a}{dt} = -\Gamma[(1 - f_0)n_a - f_0(1 - n_a)]. \tag{2.21}$$

Equation (2.21) is widely used, but probably almost never valid, because if Γ is sufficiently small for the perturbation theory to work, then the intra-adsorbate Coulomb interaction will almost always be sufficient to enforce the constraint (2.7), thus implying that Eq. (2.20) should be used instead.

A feature of the correlated system satisfying the constraint (2.7) is that the equilibrium occupation of the adsorbate, which we call n_{eq}, *does not follow simple Fermi statistics*. This can be shown directly by writing down the grand partition function for the correlated system, or alternatively by setting the time derivative in Eq. (2.20) equal to zero and solving for n. In either case the result is

$$n_{\text{eq}} = \frac{(N - N_0 + 1)}{N_0 \exp \beta \epsilon_0 + (N - N_0 + 1)}, \tag{2.22}$$

which is to be contrasted with the $U = 0$ result, $n_{\text{eq}} = N f_0$. This difference has a significant effect on the DIMET rate. One way of explaining the result (2.22) is to note that the

average number of single-particle states pushed a long way from the Fermi level by U is dependent on n itself. Indeed, a simple calculation shows that the average number of single-particle states N_s left available for fluctuating occupancies is no longer N as in the $U=0$ case, but rather

$$N_s = (1-n)(N-N_0+1) + nN_0 \qquad (2.23)$$

instead [see also Eq. (A10)].

Another important feature is that the relaxation rate is dependent on temperature and ϵ_0; it is *not equal to the rate* Γ *from one-electron theory*. This may be seen by writing (2.20) in a way that displays the rate of relaxation of the n. Using Eq. (2.22) in Eq. (2.20), we obtain

$$\frac{dn}{dt} = -\Gamma_{\text{eff}}(n - n_{\text{eq}}) \equiv -\Gamma_{\text{eff}}\delta n, \qquad (2.24)$$

where the *effective* rate Γ_{eff} is given by

$$\Gamma_{\text{eff}} = \Gamma[(N-N_0+1)f_0 + N_0(1-f_0)]. \qquad (2.25)$$

This result is also relevant for discussions of the width of the occupied (unoccupied) level on the adsorbate as might be measured by photoemission (inverse photoemission). It is noteworthy that such a measurement does not measure the Γ that would be predicted directly by electronic structure theory. This is one of the predictions of the simple SCA theory that persists to other regimes, at least qualitatively. It is certainly true that the width of the resonant level changes by a substantial factor when the Fermi level is crossed, a factor that is completely missing in the uncorrelated theory.

We now calculate the friction coefficient in the LFA. In the region of validity of the semiclassical approximation, $\Gamma \ll |\epsilon_0 - \epsilon_F|$ and the second term in Eq. (2.12) can be neglected to first order. We can write the energy transfer in this case as

$$\dot{E}_{\text{non}}(t) = \dot{\epsilon}_0(t)\,\delta n(t). \qquad (2.26)$$

As discussed earlier (see also Brunner and Langreth[28] and Head-Gordon and Tully[24]), the LFA may be obtained simply by linearizing the equations about small time differences, a procedure equivalent to calculating the force-force correlation function (see D'Agliano *et al.*[2]). Here such a procedure is trivial, and we obtain the solution of Eq. (2.24) corresponding to this as

$$\delta n = -\frac{1}{\Gamma_{\text{eff}}}\frac{dn_{\text{eq}}}{dt}. \qquad (2.27)$$

This leads to the predictions for the friction

$$M\eta = \frac{1}{\Gamma}\left(\frac{d\epsilon_0}{dz}\right)^2\left[-\frac{d}{d\epsilon_0}\left(\frac{N}{\exp\beta\epsilon_0+1}\right)\right] \qquad (2.28)$$

for $U=0$, and

$$M\eta = \frac{1}{\Gamma_{\text{eff}}}\left(\frac{d\epsilon_0}{dz}\right)^2\left[-\frac{d}{d\epsilon_0}\left(\frac{N-N_0+1}{N_0\exp\beta\epsilon_0+N-N_0+1}\right)\right] \qquad (2.29)$$

for $U=\infty$. The expression for the $U=0$ case can also be obtained simply as the small Δ limit of the phase shift expression (2.16). However, the $U=\infty$ expression, to the best

of our knowledge, has not been obtained previously. The differences in these two expressions are significant and in some cases substantial.

We conclude this subsection by noting that in cases like this, the LFA should be expected to break down unless $\beta\dot{\epsilon} \ll \Gamma$. Then one must revert to the numerical solution of the master equation simultaneously with the equations of motion on the potential curve on which the adsorbate temporally resides. But one should use the right master equation!

E. Electronic friction induced by the level width, and beyond

A different picture of electronic friction emerges for systems with large adsorbate level width $\Gamma(\sim|\epsilon_0 - \epsilon_F|)$ and small temperatures $T(\ll\Gamma)$. Electronic friction in this case arises from resonant electron tunneling induced by the adsorbate width. In this limit, the LFA should provide an excellent approximation for systems, where intra-adsorbate correlations are not important. The only time scale introduced by the substrate-adsorbate interaction then corresponds to the tunneling rate Γ. The criterion for validity of the limit can formally be expressed as a condition that $|\dot{\epsilon}/\Gamma^2|$ and $|\dot{\Gamma}/\Gamma^2|$ are much smaller than unity. Indeed, for typical values of the level width $\Gamma(\sim 1\text{ eV})$ and realistic parameterizations for the position dependence of ϵ_0 and Γ,[29] an adsorbate of unit mass satisfies the above condition up to kinetic energies of the order of an eV. At the same time, the electronic friction will show very little temperature dependence in the experimentally relevant regime, $T\ll\Gamma$.

However, it is well known from condensed matter that strongly correlated magnetic impurities in the bulk of simple metals exhibit anomalous low-temperature behavior (the Kondo effect) with origin in magnetic scattering. The spin-flip scattering of substrate electrons or holes from the uncompensated impurity spin provides an additional hybridization channel, which lowers the energy of the metal-impurity complex. The system then has a tendency to rearrange its electronic structure in order to maximize the rate of the low-energy scattering, and produces a narrow resonance (the Kondo or mixed valent states) in the local density of states, which forms near the Fermi level. The width of this resonance, of the order of the Kondo temperature T_K, depends on ϵ_0 and Δ, and is therefore a function of the adsorbate's position. The dependence of T_K on these parameters ϵ_0 and Δ has an analytical solution for the degenerate Anderson model with rectangular $\xi(\epsilon)$. Using the Bethe ansatz,[30] it is found that the Kondo temperature for the low-energy scale (called T_l there) is given by

$$T_K = \Gamma\left(1 + \frac{1}{N}\right)D_r\left(\frac{N\Delta}{\pi D_r}\right)^{1/N}\exp\left(-\frac{\pi|\epsilon|}{N\Delta}\right), \qquad (2.30)$$

where Γ is the gamma function and $D_r = e^{-1/2}D$ is rescaled[26] for the assumed parabolic shape of $\xi(\epsilon)$.

An adsorbate-substrate system can typically form these strongly correlated states at some point along the trajectory of a moving adsorbate, in contrast to the typical situation for a bulk impurity state, where the parameter ranges are restricted to those of the static binding site. The narrow resonance in the spectral density introduces long electronic time scale, which can significantly alter the analysis of the first

paragraph. It is one of the goals of this paper to examine the effects of these strongly correlated states on electronic friction.

The approximations of the previous section break down and we have to resort to the general solution of the problem described by Hamiltonian (2.6) with the constraint (2.7). We do this for open-shell adsorbates with one electron (hole) in an otherwise empty (full) shell. In the notation used in the previous section, we consider N degenerate levels with $N_0 = 1$ or $N_0 = N - 1$ depending on whether we have in mind electrons or holes, respectively.

We adopt a standard textbook technique,[31,32] the non-crossing approximation (NCA). It is a self-consistent, high-temperature approximation, which has been shown to be useful[33] to energy scales down to T_K and below by comparison with exact renormalization-group calculations for quantities that can be expressed in terms of the so-called auxiliary propagators, as can be done here (see Appendix A). The NCA has been extended to the nonequilibrium situation by Langreth and Nordlander,[27] and solved numerically by Shao, Langreth, and Nordlander,[26] where the details are given. We outline the method below, and give details of this specific application in Appendix C.

The constraint (2.7) is effected by introducing an auxiliary (slave) boson,[34] which is created whenever an electron is transferred from the adsorbate level complex to the metal or destroyed in the opposite process. The operator that does this is $\alpha_a = b^\dagger c_a$, where $b^\dagger$ is the boson creation operator. The bosonized form of the effective Hamiltonian (2.5) is

$$H(t) = \sum_a \epsilon_0(t) n_a + \sum_k \epsilon_k n_{ka} + \sum_{ak} [V_{ak}(t) c_{ka}^\dagger b^\dagger c_a + \text{H.c.}].$$

$$(2.31)$$

The quantity $Q_B \equiv n_B(t) + n(t)$, where $n(t)$ is defined in Eq. (2.8), and is here just the total number of electrons in the open shell. Q_B commutes with Eq. (2.31), so that the total number of electrons $n(t)$ in the shell plus the number of bosons $n_B(t) = \langle b^\dagger b \rangle$ is conserved, and the subspaces of the Fock space with definite Q_B are disjoint. The physical subspace on which the Hamiltonian must be diagonalized corresponds to $Q_B = 1$.

The approach to solving Eq. (2.31) is based on the Green's function method developed by Kadanoff and Baym[35] and Keldysh.[36] The details of the method and description of the exact numerical solution are discussed in Langreth and Nordlander,[27] and Shao et al.[26]

III. RESULTS AND DISCUSSION

In this section, we present a comprehensive numerical study of electronic friction and its various limits as discussed in the previous two sections. We demonstrate the many-body effects by studying different models of adsorbate-metal systems.

A. Discussion of the correlation effects of simple molecules adsorbed on simple metals

Ignoring the intra-adsorbate correlations seems like a justifiable approximation for the CO molecule on metals like Pt, Pd, and Cu. This is because the typical work functions of these metals are in the range $4.5 - 6$ eV. An isolated CO molecule has a closed 2π shell with ionization potential of ~ 14 eV. In the adsorbed form, this level is deep below the Fermi energy. The negative ion state with an electron in the $2\pi^*$ orbital lies about an electron volt above the Fermi level. It is this negative ion resonance that is active in the energy transfer. The Coulomb interaction in this empty orbital regime plays a minor role since the level occupation is small ($\ll 1$).

The NO molecule adsorbed on these metal surfaces forms a very different system. An isolated NO has an additional uncompensated electron in the $2\pi^*$ orbital. Typically when adsorbed on the above metals the spectral density shows a negative ion peak an eV or so above the Fermi level, while the positive ion peak is typically several eV below the Fermi level [for example, on Cu(111) these two numbers are 1.3 eV and 2.5 eV, respectively[37]]. Since the level widths are believed to be comparable to or smaller than the separation of the nearer of these two peaks from the Fermi level, and much smaller than the separation of the farther peak, it is reasonable to use the $U = \infty$ description of the negative ion resonance to model the situation. This view is further strengthened by the experimental evidence found by Ertl's group[38] for the paramagnetism of NO on several of these surfaces. In fact Yoshimori[39] has already argued that NO on Cu(111) is a Kondo system, although in this case with a rather low Kondo temperature (~ 8 K). A system of particular interest because of the hot-electron desorption experiments is NO/Pd(111), which has been extensively modeled by Brandbyge et al.[18] assuming that a $U = 0$ description is valid. They used alternately the assumption of level width induced friction as in model A and thermally induced friction as in model B [see Eqs. (3.1) and (3.2), and below] as limiting cases, in the absence of perfect knowledge of the actual parameters. Here we solve these models with the identical parameters, but assuming instead that the $U = \infty$ description is valid. We find in each case that the friction is substantially different.

B. Spectral functions

We consider open shell adsorbates with a single electron (hole) in an otherwise empty (filled) shell as described in Secs. II D and II E, that is we take $N_0 = 1$. In the main body of this paper we follow Brandbyge et al.[18] and model the adsorbate's level position and level half-width variation, respectively, by

$$\epsilon_0 = \epsilon_\infty - C e^{-ax}, \qquad (3.1)$$

$$N\Delta = \Delta_0 e^{-bx}, \qquad (3.2)$$

where x is measured from the equilibrium position of the adsorbate. We define two models: A and B, similar to those of Ref. 18. For both models we take $\epsilon_\infty = 5$ eV, $C = 3.5$ eV, $a = 0.45$ a.u., and $b = 1.0$ a.u. For model A, $\Delta_0 = 1.5$ eV, while for model B, $\Delta_0 = 0.12$ eV. The choice (3.1) is similar to the possibly more realistic (and more slowly varying) image potential form,

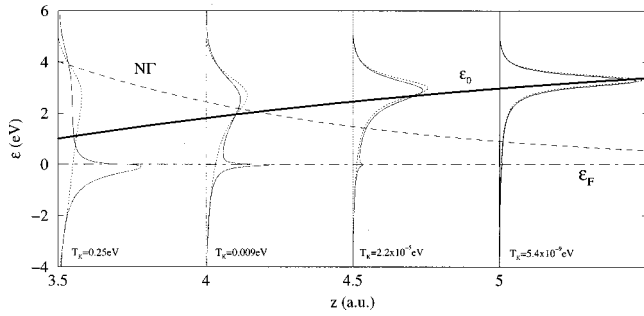$$\epsilon_0 = \epsilon_\infty \pm \frac{e^2}{4|z - z_{\text{image}}|}. \qquad (3.3)$$

FIG. 3. The total adsorbate spectral densities at different distance from the surface for the model A [see Eqs. (3.1) and (3.2), and below]. The dotted and solid lines correspond to the nondegenerate $U=0$ and doubly degenerate $U=\infty$ models, respectively, at temperature $T=0.001$ Hartree (316 K).

If we take the $z_{image}=1$ a.u., and the other parameters as above, then Eqs. (3.1) and (3.3) have Fermi-level crossings at the same place if we take the minus sign in Eq. (3.3) and $z=x+3.8$ a.u., a definition that we take throughout this paper. We will present some calculations using Eq. (3.3) in the Appendix.

We will first discuss the model A. Its parametrization [see Eqs. (3.1) and (3.2), and below] is illustrated in Fig. 3. It corresponds to the regime of friction induced by level width, in which the adsorbate level width is much larger than temperature and of the same order as the energy difference $|\epsilon_0 - \epsilon_F|$.

In Fig. 3, we show the spectral function for this model at several distances from the surface. The dotted lines correspond to the uncorrelated system ($N=1$, $U=0$) and solid lines correspond to a doubly degenerate correlated ($N=2$, $U=\infty$) system at temperature $T=0.001$ Hartree (316 K). We should note that we keep $N\Delta$ constant in calculations comparing the same systems with different degeneracy N, since such approach produces comparable level widths and spectral densities, as suggested by Eq. (2.25). For the same reason, when comparing $U=\infty$ with $U=0$ results, we normally will take $N=1$ for the $U=0$ results, irrespective of what the actual value of N is.

The correlated states are characterized by the appearance of narrow Kondo resonance in the spectral function near ϵ_F. Its energy (measured from ϵ_F) and width are of the order of the Kondo temperature T_K. As the system parameters vary along the adsorbate trajectory, so does the Kondo temperature T_K. We show the position dependent Kondo temperature, calculated from Eq. (2.30), inside of each panel in Fig. 3. Far from the metal surface ($z=5$), T_K is much smaller than the substrate electron temperature T and the Kondo resonance is destroyed by the high temperature. There is thus very little difference between the $U=0$, $N=1$ spectral function and the correlated one at the actual value of N. Closer to the surface (between $z=3.5$ and $z=4$ a.u.), $T_K \sim T$ and the system exhibits the anomalous logarithmic temperature behavior known as the Kondo effect. The spectral weight shifts from the broad resonance of width $N\Gamma$ centered at ϵ_0 towards the Kondo peak near ϵ_F. Even closer to the surface, where $T_K \gg T$, the Kondo resonance sharpens further and becomes temperature independent, although this regime is not fully accessible via the NCA.
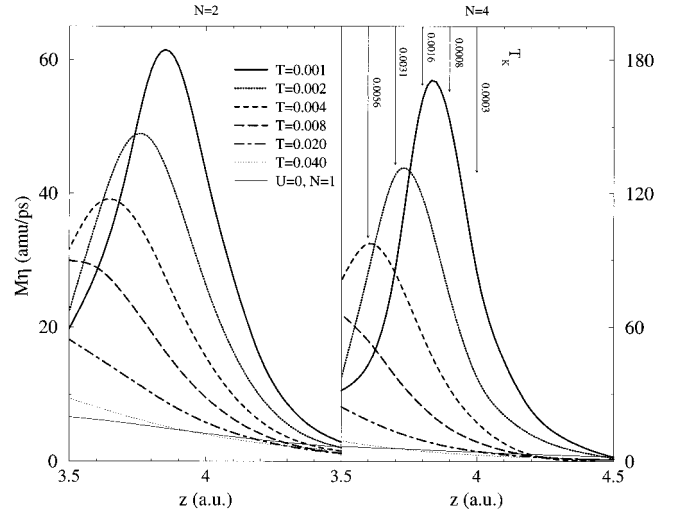

FIG. 4. Electronic friction $M\eta$ in the LFA limit as a function of the adsorbate-substrate separation z. The $N=1$ curve corresponds to friction of the noninteracting, nondegenerate system. Its temperature is not shown, as it is essentially temperature independent in the range shown. The left panel shows $N=2$ and right panel $N=4$ degenerate system. All temperatures are in atomic units [0.001 a.u. =316 K].

The NCA allows us to treat the case $N_0=1$ for electrons (or $N_0=N$ for holes). Other values of N_0 have been studied in the equilibrium case,[40] and have Kondo-like resonances in their spectral functions for *either* position of the level with respect to the Fermi level in Fig. 2 with Kondo temperatures given by expressions similar to Eq. (2.30). Application of the $N_0=1$ results for the open-shell Fermi-level position to such cases is therefore perhaps a viable option, qualitative at best, but still likely to give more reasonable results than the $U=0$ models often used. It would obviously be desirable if a nonequilibrium theory specifically for $N_0 \neq 1$ could be developed.

C. The LFA limit

The corresponding, position dependent friction for the model A at $v \rightarrow 0$ is shown in Fig. 4. The quantity plotted here is the electronic friction normalized to unit mass (amu =atomic mass unit) $M\eta \equiv \dot{E}/v^2$. The $U=0$, $N=1$ system has a friction (as shown in the figure) which is to a large degree independent of temperature and slowly varying with position. It is increasing as the level ϵ_0 approaches the Fermi level. Its value at the equilibrium position, $z_0 \sim 3.8$ a.u., of the NO (CO) molecule adsorbed on the metal is in agreement with that used by Brandbyge *et al.*,[18] as long as the degeneracy factor of 4 is taken into account (they use $U=0$, $N=4$).

The interacting system ($U=\infty$) shows a considerably enhanced electronic friction in the region between $z=3.5$ and $z=4.5$ a.u., right in the region where the adsorbed species are expected to spend most time. We compare frictions of a twofold degenerate ($N=2$) system (left panel) and a fourfold degenerate ($N=4$) system with identical tunneling rate $N\Gamma$. The much larger frictions at $N=4$ are result of the fact that more spectral weight is concentrated in the Kondo peak and the relative importance of the correlated state is thus in-

creased. An adsorbate system with $N=4$ and with the mass of the NO or CO molecule (~ 30 amu) has a large electronic friction $\eta=5.4$ ps^{-1} at room temperature and the equilibrium position z_0. In contrast, for the $U=0$, $N=1$ system, $\eta=0.25$ ps^{-1} at the same position.

1. Region of maximum friction enhancement

In the absence of correlations, large frictions occur in the spatial region where the adsorbate resonance is near the Fermi level. The rapid charge fluctuations in and out of the adsorbate level in this region create electron-hole excitations in the metal, which produce the nonadiabatic effects responsible for the dissipative energy transfer.

On the other hand, the position of the maximum many-body enhancements is given by the condition $T_K(z) \sim T$ where the nonadiabatic effects of the correlated states are most pronounced. This can be understood in terms of properties of the Kondo resonance. Its width (γ) and position (measured from ϵ_F) are of the order of T_K for not too high temperatures ($T \lesssim T_K$). As the local environment changes with the adsorbate motion, so does the equilibrium electronic configuration. The rate of this change is characterized by $\dot{T}_K$. Under dynamic conditions, electrons rearrange in response to the dynamic perturbation according to the Kondo-induced relaxation time, which is of the order of the inverse Kondo resonance width γ. The resulting nonadiabaticity is characterized by the rate $R_K = \dot{T}_K/T_K$. However, at $T_K \ll T$, temperature broadens the Kondo peak and the width is $\sim T$ rather than $\sim T_K$. The nonadiabaticity at high temperatures is thus characterized by $\dot{T}_K/T$ ($\ll R_K$), and the friction is smaller there. At $T_K \gg T$, one enters the Fermi-liquid-like region,[41] which is again describable by Eq. (2.16),[5] with $\delta = n\pi/N$. In the extreme Kondo region where $n \approx 1$, so that δ is roughly independent of system parameters, one expects a very small friction again. Although this region is not fully accessible to the NCA, nevertheless our results show the expected falloff as T_K becomes greater that T.

The arrows in the right panel of Fig. 4 show the values of T_K (in a.u.) at different positions, and demonstrate that the largest enhancement occurs where T_K passes through the electronic temperature T. Since T_K is only weakly dependent on N, the position of maximum friction is essentially the same in both panels. We must stress, however, that the condition for maximum friction enhancement need not always coincide with that for maximum friction. This is because the total friction also contains a contribution from the conventional mechanism. If such a contribution is not small, maximum friction will occur at a position closer to where the adsorbate level passes through the Fermi energy. This is the case at higher temperatures (Fig. 4), particularly for the $N=2$ system, the friction of which is less dominated by the correlated states. At temperatures $T \gg T_K$, the friction converges to that of the noninteracting system with appropriate width, and becomes independent of N.

2. Temperature effects

The dramatic and anomalous temperature dependence is consistent with the notion of the Kondo-induced nonadiabaticity. The width of the Kondo peak in the region of large
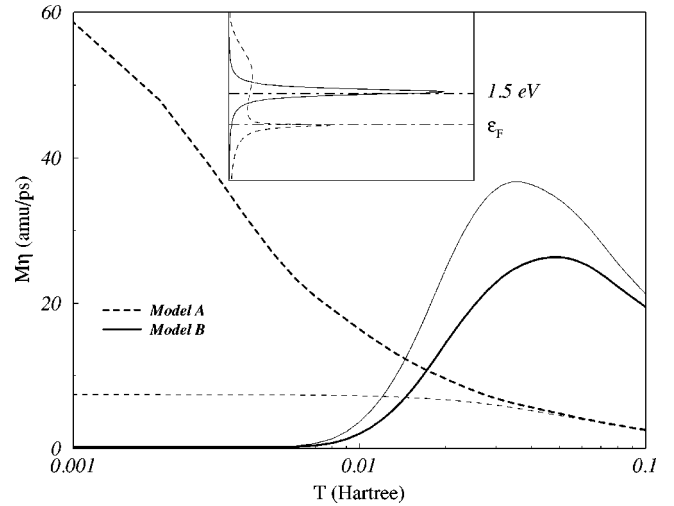

FIG. 5. Temperature dependence of the friction $M\eta$ in the LFA limit at $z=3.8$ a.u. for model A (dashed lines) and model B (full lines). The thin and bold lines correspond to the nondegenerate $U=0$ and doubly degenerate $U=\infty$ models, respectively.

friction is of the order of temperature T by virtue of the condition discussed in the previous section. The resonance is thus narrower at lower temperatures, and produces a longer electronic time scale, larger nonadiabaticity, and larger frictions. At the same time the friction is strongly position dependent and, therefore, is not necessarily a monotonic function of temperature at a given position.

In scattering or sticking experiments, the electronic frictions of model A produce energy losses that are only a small fraction of the maximum kinetic energy of the scattering atom or molecule.[42] However, the outcome of adsorption or reaction processes is determined by values of friction at the equilibrium position in the potential well, where the adsorbate spends most of its time. If the equilibrium position coincides with the region of large friction, the electronic degrees of freedom can significantly enhance the desorption rates. Moreover, if the adsorbate is in the strongly correlated regime, as defined above, the desorption could show strong and anomalous temperature dependence. This is illustrated in Fig. 5 where we show the temperature dependence of the friction $M\eta$ at $z=3.8$ a.u. for the $N=2$ model A (dashed lines). In the absence of the Coulomb repulsion, η shows very little temperature dependence in the experimentally interesting temperature range ($T \lesssim 0.02$ Hartree ~ 6000 K). In contrast, the interacting system has strongly temperature-dependent friction exactly in this temperature range with the largest enhancement at low temperatures. It is easy to understand why the friction decreases with increasing temperature. The Kondo resonance broadens with temperature and the electronic time scales become shorter. This leads to reduced nonadiabaticity and smaller friction. One should note, however, that the behavior is not always a monotonic falloff as here. Inspection of Fig. 4 shows that at closer distances to the surface, the friction will *increase* rapidly with temperature before it falls off.

One issue that needs further investigation before a quantitative application to the hot electron induced desorption problem is the question of how a *time-dependent* electron temperature affects the results. We have a large friction that

comes from a sharp resonance, so that the friction will presumably not effectively reach its value at the peak temperature instantaneously as the electron temperature is raised. One might then expect this would enhance the desorption even more, since the friction would tend to remain at its initial, in many cases higher value, during a part of the crucial time period. If this argument is correct, then the desorption should occur extremely quickly, because the period of highest friction would be limited to short time after the temperature rise.

Experimental verification of the Kondo-induced friction should be possible if the heating curve of substrate electrons is short on the Kondo time scale ($\sim$ inverse width of the Kondo resonance). In such a case, the friction at peak electronic temperature should carry information about the initial equilibrium conditions, e.g., the initial ambient temperature. The desorption yield should then exhibit strong, logarithmic dependence on the initial substrate temperature. Depending on the value of the Kondo temperature at the equilibrium position of the adsorbate (see Fig. 4), the desorption yield can either increase or decrease with the initial substrate temperature. We estimate, for T_K of order of room temperature, the laser pulse duration needs to be <0.2 ps. It can be even longer for lower temperatures, but shorter for higher temperatures.

The desorption yield should also be sensitive to the speed at which the temperature of substrate electrons rises during the laser heating (on the Kondo time scale), because the actual friction will be unable to follow the adiabatic friction versus temperature curve. For the situation in Fig. 4, the desorption yield should increase with the slope of the heating curve, as the friction at peak electron temperature would have a higher value, characteristic of the previous lower temperature.

Other promising experiments for direct confirmation of the Kondo induced friction enhancements are the measurements of vibrational line shapes of adsorbed molecules. The damping should show strong and anomalous temperature dependence near the Kondo temperature of the system. We plan to investigate this issue thoroughly in a later publication.

3. Comparison of the many-body enhancement with the traditional mechanism for friction

So far, we have only demonstrated the importance of the intra-adsorbate Coulomb repulsion for an adsorbate-metal complex in the magnetic state and with the adsorbate level shifted by the adsorbate-metal interaction towards ϵ_F. In this section, we discuss in detail the conditions that lead to large many-body enhancements.

Two conditions have to be satisfied for the enhancement to be large. First of all, the correlated states must form somewhere on the adsorbate trajectory opening up the additional nonadiabatic channel. Second, the Kondo temperature characterizing these states must change rapidly on time scales given by the Kondo resonance ($\sim T_K^{-1}$).

The second condition is ideally realized in systems such as the model A (Fig. 3), in which ϵ_0 shifts towards ϵ_F on approaching the surface, so the magnitude of $|\epsilon_0 - \epsilon_F|$ decreases when $|\Delta|$ increases. Under this scenario, the Kondo temperature [Eq. (2.30)] may change rapidly even if the parameters ϵ_0 and Δ do not. The nonadiabaticity induced by the electron interactions is then large compared with the conventional source of nonadiabaticity, characterized by the rates $R_\Gamma = \dot{\Gamma}_a/\Gamma$ and $R_\epsilon = \dot{\epsilon}_a/\Gamma$ evaluated near the Fermi-level crossing. For example, $R_K/R_\epsilon = 9.6$ and $R_K/R_\Gamma = 7.8$ for the model A at the distance $z = 3.8$ a.u., where $T_K \sim 0.001$ and where the maximum friction occurs at that temperature. Another way to understand the large frictions is to realize that the two contributions in Eq. (2.15) add up constructively under these circumstances.

Qualitatively different behavior occurs in systems with the adsorbate resonance shifting away from the Fermi level as the surface is approached. In this case, the two contributions in Eq. (2.15) have opposite sign. If both of the contributions are large, and none of them dominant, the resulting friction will necessarily be small. An equivalent statement follows from exploring the position dependent Kondo temperature. The exponent in expression (2.30) varies much more slowly than in the previous case and produces thus smaller deviations from equilibrium under identical equilibrium conditions.

We demonstrate these issues on two model systems in detail in Appendix D where we also discuss the many-body effects in regions where the traditional mechanism produces large frictions.

4. DIMET and semiclassical approximation

So far, we have discussed cases in which the large frictions are produced by low-energy electron-hole excitations. These processes dominate the energy transfer whenever the width of the adsorbate resonance is comparable with its distance from the Fermi level. In the DIMET regime, the desorption is induced by multiple transitions between the metal and the adsorbate of hot, nonequilibrium electrons thermally excited in the substrate by laser pulses. We demonstrate such situations on model B [see Eqs. (3.1) and (3.2), and below] similar to model A but with smaller width $\Delta \rightarrow 0.08\Delta$. We choose this parameterization so that a comparison with Brandbyge et al.[18] is possible. Figure 5 shows the calculated frictions versus temperature at $z = 3.8$ a.u. for model A (dashed lines) and model B (full lines). The inset highlights the differences in spectral functions between the two cases. The broad resonance of model A produces almost temperature-independent friction in the absence of the correlations U. As we noticed earlier, the introduction of the intra-adsorbate Coulomb repulsion leads to Kondo-enhanced energy transfer with strong temperature dependence.

In model B, virtually no friction exists for $T \ll \epsilon_0$. However, at high enough temperatures ($T \sim \epsilon_0$) the friction becomes large and temperature dependent even in the absence of the interaction U. This is because the narrow width Γ introduces a long electronic time scale and, consequently, large nonadiabaticity when excitations into the level are possible, i.e., at $T \sim |\epsilon_0|$.

The effect of electron correlations at higher temperatures can be discussed in simple terms because this regime is well described by the SCA limit. In fact, the friction of model B in Fig. 5 is accurately reproduced by the analytic expressions (2.28) and (2.29).
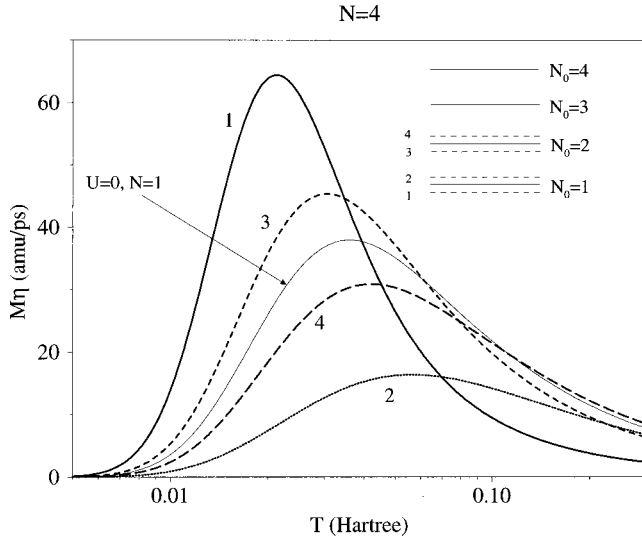
FIG. 6. Temperature dependence of the friction $M\eta$ in the LFA limit of the semiclassical approximation. Each curve shows the friction for specific position of ϵ_F (indicated by dashed lines in the legend) with respect to the $N=4$ adsorbate level complex. We normalize the effective width Γ_{eff} so that all cases shown here have identical width $\Gamma=0.12$ eV at zero temperature. The cases plotted are (1) $N_0=1$, $\epsilon_0=1.5$ eV; (2) $N_0=1$, $\epsilon_0=-1.5$ eV; (3) $N_0=2$, $\epsilon_0=1.5$ eV; (4) $N_0=2$, $\epsilon_0=-1.5$ eV; and $U=0$ the corresponding $N=1$ noninteracting system. ϵ_0 is measured from the Fermi energy.

Here we parametrize our models in a way that keeps $N\Gamma$ fixed in comparing systems with different N. This ensures that at $T=0$, $\Gamma_{\text{eff}}=N\Gamma$ is identical to the width of the $U=0$ model. As $T\to\infty$, $\Gamma_{\text{eff}}\to[(N+1)2]\Gamma$, i.e., $\frac{3}{2}\Gamma$ for the $N=2$ system shown in Fig. 5. The smaller width of the interacting system eventually leads to larger friction as $T\to\infty$. If we replace $\Gamma\to\Gamma_{\text{eff}}$ in Eq. (2.28) to make the $U=\infty$ and $U=0$ systems spectroscopically equivalent at all temperatures, then the friction of the $U=\infty$ system is always *suppressed* relative to the $U=0$ system at the same N, except for the uninteresting closed-shell cases, where the $U=0$ and $U=\infty$ cases have the same friction.

In Fig. 6, we show the solution of the analytic master equation results in the SCA approximation [Eqs. (2.20) and (2.21)]. We compare the friction of the $N=1$ noninteracting adsorbate and of the interacting $N=4$ adsorbates for four different Fermi-level positions as described in the caption to the figure. The comparison is done by normalizing the effective adsorbate level width in each case to $\Gamma=0.12$ eV at low temperature. The cases labeled (1) and (3) in the figure most closely describe CO and NO on Pd(111) and similar surfaces, respectively.

In the vicinity of the threshold of DIMET activation, $T\sim0.01$ Hartree in the illustrated case, the friction varies as $\exp(-|\epsilon_0|/T)/T$ for all models. It is then a fair question to ask what number N_{eff} one should multiply the $U=0$, $N=1$ friction by to get the correct $U=\infty$ friction. Brandbyge *et al.*[18] implicitly assumed that $N_{\text{eff}}=N$. A simple calculation yields $N_{\text{eff}}=(N-N_0+1)/N_0$ for $\epsilon_0>\epsilon_F$ and $N_{\text{eff}}=N_0/(N-N_0+1)$ for $\epsilon_0<\epsilon_F$. This leads to a *suppression* factor N_{eff}/N of 1/4 in the open-shell $N=2$ case, and 1/16, 3/8, and 1/6 for the three open-shell $N=4$ cases labeled 2, 3, and 4, respectively,
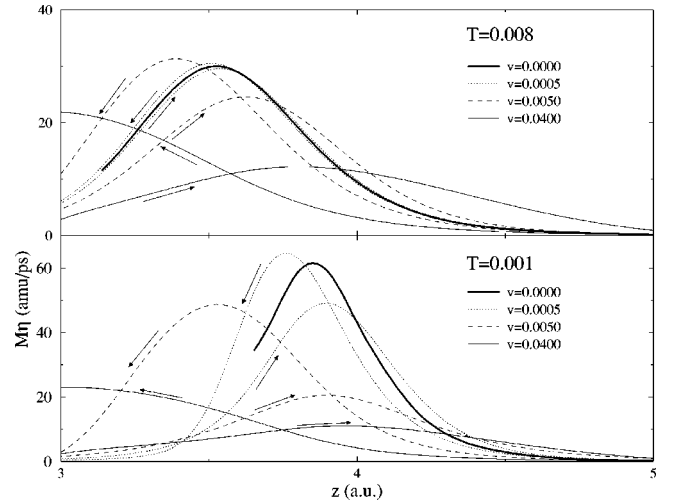

FIG. 7. $M\eta$ of the doubly degenerate model A at temperatures $T=0.001$ (316 K) and $T=0.008$ (2420 K) is plotted for different velocities (v) of adsorbate motion. Arrows indicate the direction of motion.

in Fig. 6. For the closed shell cases, on the other hand, there is no suppression in this region, that is $N_{\text{eff}}/N=1$.

D. Finite velocities

The results presented in Fig. 4 are based on a linear response theory calculations—a generalization of the susceptibility calculations discussed by Brunner and Langreth.[28] Calculations of the full susceptibility are interesting in their own right as they allow a comparison of the contributions from varying Γ and ϵ_0. We will discuss the details in a separate publication. However, an important issue needs to be addressed here in connection with the large frictions found in the LFA limit (Fig. 4). Namely, can these enhancements survive the dynamic effects of finite velocities? The answer is far from obvious. As demonstrated by Figs. 3 and 4, the spatial extent of the region with strong correlations is very limited. The time required to form the narrow Kondo resonance is of the order of $\sim T_K^{-1}$. If the adsorbate traverses this spatial region in less than this characteristic time, the effects are likely to be destroyed.

At finite velocities, the frictional dissipation is a functional of the adsorbate's trajectory. To simplify the interpretation of the results we picked trajectories with constant adsorbate speed, and have arbitrarily taken them to start at infinity, with the adsorbate approaching as near as $z=2.5$ a.u. to the surfaces, then reversing direction, and proceeding outward to $z=\infty$ again. The main features are shown in Fig. 7, where, for the $N=2$ model A and at temperatures $T=0.001$ and $T=0.008$ Hartree, we plot the friction $M\eta$ at 3 different velocities, $v=0.0005$, 0.005, and 0.04 a.u., with arrows indicating the direction of the adsorbate motion. The friction in the LFA limit (bold) is also shown except for the smallest z values, where NCA breakdown began to occur. The main effect at low velocities is the development of a hysteresis in the friction along the direction of motion as the electronic configuration adjusts to local conditions with certain lag time. Generally, on the inward trajectory the adsorbate experiences larger friction because the largest nonadia-

baticity occurs closer to the surface where the $\epsilon_0(z)$ and $\Gamma(z)$ curves are steeper. The Fig. 7 also demonstrates the approach to the LFA limit is temperature dependent. For instance, at $v = 0.0005$ a.u., the friction is well described by its LFA limit at $T = 0.008$ while significant deviations already exist at $T = 0.001$. The cause of the temperature dependence can be traced to the width ($\gamma \sim T$) of the Kondo resonance, which is about eight times smaller at $T = 0.001$ than it is at $T = 0.008$. Thus it takes a longer time for the resonance to form at lower temperatures and hence the larger deviations from the LFA limit.

A further increase in velocity affects the formation of the Kondo peak, erasing its effect almost completely at $v = 0.04$ for $T = 0.001$. Although no abrupt crossover from the high to low friction regime exists, significant enhancement persists to velocities $v \sim 0.005$ a.u. even at room temperature. These velocities correspond to kinetic energy $E \sim 19$ eV for an adsorbate with mass $M \sim 30$ amu.

Two competing factors thus affect the Kondo-enhanced friction at finite velocities. On one hand, more rapid variation in T_K in a region where $T_K \sim T$ leads to stronger frictions in the LFA limit. At the same time, the large $\dot{T}_K$ limits the spatial extent of the Kondo region and consequently slower velocities will destroy the many-body enhancement. However, our calculations indicate that even systems with extremely rapid variation of the Newns parameters have strong frictions persisting to experimentally interesting values of kinetic energies.

IV. CONCLUSIONS

We have studied the influence of strong intra-adsorbate Coulomb correlations on electronically induced energy transfer between metallic surfaces and atom or molecular adsorbates moving outside of the metal. Although we considered specific models of adsorbate-metal systems in our numerical calculations, the most general conclusions presented in this paper apply to many different electronically activated surface processes. We summarize those conclusions here.

We have shown that open-shell atoms and molecules in interaction with metals can experience electronic frictions much stronger than predicted by the traditional mechanism. The necessary condition for such an enhancement to occur is that the Kondo temperature be of the same order of magnitude as the physical temperature of the substrate conduction electrons. Maximum enhancement in the LFA ($v \to 0$) limit occurs at a distance from surface where the position-dependent Kondo temperature $T_K(z) \sim T$. This point is typically closer to the equilibrium position of the adsorbate, than for the traditional mechanism. The magnitude of the friction enhancement at that point is proportional to the time variation of T_K relative to the low-energy scale given by the Kondo peak width, i.e., $[\sim (\dot{T}_K / T_K)]$.

The main effect of velocity is (i) to shift the region of large friction along the direction of adsorbate motion, and (ii) to reduce the Kondo enhancement. However, significant enhancements are found at kinetic energies large enough to be considered important under typical conditions.

Away from the Kondo region, the main many-body effects are traced to two properties of the strongly correlated $U = \infty$ systems. First, the average number of single-particle states available for fluctuating occupancy, rather than being the constant N as in the $U = 0$ case, is a function of the level occupation, which increases as the occupation decreases. This in turn leads to an occupation probability whose energy derivative has a smaller magnitude than that of N times the Fermi-Dirac distribution. This implies smaller nonadiabiticity and friction in the $U = \infty$ case. The second effect comes from the changing width of the adsorbate resonance between $N\Gamma$ when the level is fully (singly) occupied and Γ when it is empty. The electronic time scales thus change with the level occupation, and hence temperature and level positions.

APPENDIX A: PHYSICAL PROPAGATOR AND SPECTRAL DENSITIES

In this appendix, we present definitions and identities relevant to the theoretical formulation of energy transfer within the NCA for open-shell systems with one electron (hole) in an otherwise empty (full) shell. In the slave boson technique used here, the propagation of the real electron is described in terms of a two-particle Green's function,

$$iA_a(t,t') = \langle T_C \alpha_a(t)\alpha_a^+(t')\rangle, \tag{A1}$$

where the operators $\alpha_a(t) = b^\dagger(t)c_a(t)$ and the symbol T_C orders all operators according to their position on a contour C in the complex time plane, which can be taken to be the Kadanoff-Baym contour,[35] the Keldysh contour,[36] or a more general choice. $A_a(t,t')$ can be diagrammatically expanded in terms of single-particle Green's functions,

$$iG_a(t,t') = \langle T_C c_a(t)c_a^\dagger(t')\rangle$$

and

$$iB(t,t') = \langle T_C b(t)b^\dagger(t')\rangle, \tag{A2}$$

which are merely auxiliary quantities in this formulation. The NCA expression for the physical electron propagator consists in making the factorization

$$A_a(t,t') \approx iG_a(t,t')B(t',t), \tag{A3}$$

while throwing away the spurious terms introduced thereby that would come from the wrong part of the Fock space. Then a standard analytic continuation onto the real-time axis allows us to relate the analytic pieces $A^> = \langle \alpha_a(t)\alpha_a^\dagger(t')\rangle$ and $A^< = \langle \alpha_a^\dagger(t')\alpha_a(t)\rangle$ to those of the auxiliary Green's functions (A2). These are

$$A_a^>(t,t') = g_a(t,t')B^<(t',t),$$
$$A_a^<(t,t') = G_a^<(t,t')b(t',t), \tag{A4}$$

where $g_a(t,t') = G_a^>(t,t') + G_a^<(t,t')$ and $b(t,t') = B^>(t,t') - B^<(t,t')$. The advanced and retarded Green's functions are

$$A_a^{A,R}(t,t')=G_a^{A,R}(t,t')B^<(t',t)-G_a^<(t,t')B^{R,A}(t',t).$$
(A5)

Following Kadanoff and Baym,[35] we introduce new time variables $\frac{1}{2}(t+t')\rightarrow t$ and $(t-t')\rightarrow \tau$, and perform the Fourier transform,

$$A_a^<(\omega,t)=\int_{-\infty}^{\infty}d\tau e^{i\omega\tau}A_a^<(t+\tfrac{1}{2}\tau,t-\tfrac{1}{2}\tau),$$
(A6)

and similarly for $A_a^>$. The spectral density of states at time t is then[35]

$$\rho(\omega,t)=\frac{N}{2\pi}[A_a^>(\omega,t)+A_a^<(\omega,t)]=-\frac{N}{\pi}\mathrm{Im}A^R(\omega,t),$$
(A7)

and the Wigner distribution function for the level occupation (2.13) used in Eq. (2.15) is

$$n_a(\omega,t)=\frac{1}{2\pi}A_a^<(\omega,t).$$
(A8)

The sum rule on the spectral function, however, is different from that for the noninteracting case because of the nonfermionic equal time anticommutation relations

$$\{\alpha_a(t),\alpha_a^\dagger(t)\}_+=c_a^\dagger(t)c_a(t)+b^\dagger(t)b(t),$$
(A9)

which lead to the following expression for the number of single-particle states,

$$N_s(t)=-N\int_{-\infty}^{\infty}\frac{d\omega}{\pi}\mathrm{Im}A_a^R(\omega,t)=N-(N-1)\langle n(t)\rangle,$$
(A10)

with $\langle n(t)\rangle=\Sigma_a\langle n_a(t)\rangle=N\langle n_a(t)\rangle$, in agreement with Eq. (2.23) when $N_0=1$.

The principal error in the NCA comes from the factorization (A3), that is in going from the auxiliary functions $G_a^<$ to the physical functions $A_a^<$.[33] Here we show that the two integrals over $A_a^<$ that occur in the energy expression (2.15) are the same as those over the auxiliary function $G_a^<$, even when the factorization approximation (A3) is not made. Thus we are able to circumvent the principal NCA error in the actual friction calculations, although not in the calculations of spectral functions. Fortunately, the latter are used for interpretative purposes only.

The first integral in question expresses the probability that the adsorbate state is occupied at time t and is given by

$$\langle n(t)\rangle=N\int_{-\infty}^{\infty}\frac{d\omega}{2\pi}A_a^<(\omega,t)=N\int_{-\infty}^{\infty}\frac{d\omega}{2\pi}G_a^<(\omega,t).$$
(A11)

The second equality in Eq. (A11) is simply the consequence of the equal time commutation relation $[b,b^+]=1$ and the constraint (2.7) on the Fock space.

The second integral in question involves the first moments, for which we similarly can prove the following identity:

$$\int_{-\infty}^{\infty}\frac{d\omega}{2\pi}\omega\ A_a^<(\omega,t)=\int_{-\infty}^{\infty}\frac{d\omega}{2\pi}\omega\ G_a^<(\omega,t).$$
(A12)

This is done by realizing that the integral in Eq. (A12) is equal to

$$\left(\mathrm{Im}\frac{\partial A_a^<(t,t')}{\partial t'}\right)_{t=t'}.$$
(A13)

The differentiation of $A^<(t,t')$ produces two terms, one of which is zero due to the constraint (2.7). The other one yields

$$\left(\mathrm{Im}\frac{\partial G_a^<(t,t')}{\partial t'}\right)_{t=t'},$$
(A14)

which again follows from the equal time commutation relation $[b,b^+]=1$ and the constraint (2.7). This completes the proof that the auxiliary functions give the same results in Eq. (2.15) as the physical ones.

One can also prove by a similar method that the more approximate $A_a^<$ of Eq. (A4) obtained by making the factorization (A3) will also give the same result when used in the energy expression (2.15). This means that even the physical functions obtained with the approximation (A4) will give the same value to the energy expression (2.15) as the auxiliary functions obtained directly from the solution of the coupled NCA equations.

APPENDIX B: DERIVATION OF ENERGY TRANSFER EXPRESSION

In this appendix, we review basic identities of time dependent formalism at finite temperatures and show the details of derivation of the expression (2.12) for energy transfer.

Let us assume the system is in equilibrium until time t_0 when the perturbation is switched on. The thermal average $\langle A\rangle=\mathrm{Tr}\{\rho_0 A\}$ of an operator A before t_0 can be conveniently evaluated in the basis $\{|n\rangle\}$ in which the Hamiltonian $H(t_0)$ is diagonal. Then

$$\rho_0=e^{\beta\Omega}\sum_n e^{-\beta(E_n-\mu N)}|n\rangle\langle n|,\ \ e^{-\beta\Omega}=\sum_n e^{-\beta(E_n-\mu N)},$$
(B1)

where $H(t_0)|n\rangle=E_n|n\rangle$ and Ω is the grand canonical potential. The time evolution of states $|n(t)\rangle$ under the action of the time dependent Hamiltonian $H(t)$ is

$$|n(t)\rangle=U(t,t_0)|n\rangle,\quad U(t,t_0)=T\exp\left\{-i\int_{t_0}^t d\tau H(\tau)\right\}.$$
(B2)

The density operator $\rho_0(t)=e^{\beta\Omega}\Sigma_n e^{-\beta(E_n-\mu N)}|n(t)\rangle\langle n(t)|$ thus becomes time dependent for $t>t_0$ with the time evolution governed by the quantum Liouville theorem. However, we will use the Heisenberg picture operator $A_H(t)\equiv U(t_0,t)A U(t,t_0)$ and write the expectation value

$$\langle A(t)\rangle = \mathrm{Tr}\{\rho_0 A_H(t)\} = e^{\beta\Omega} \sum_n e^{-\beta(E_n - \mu N)} \langle n|A_H(t)|n\rangle \tag{B3}$$

with all the time dependence assembled into the operator $A_H(t)$. The energy transfer per unit time can thus be straight-forwardly calculated according to the formula

$$\dot{E}(t) = \frac{d}{dt}\mathrm{Tr}\{\rho_0 H_H(t)\} = \mathrm{Tr}\left\{\rho_0 \frac{\partial H_H(t)}{\partial t}\right\}. \tag{B4}$$

For the time-dependent Anderson Hamiltonian (2.31), this becomes

$$\dot{E}(t) = \sum_a \left[\dot{\epsilon}_a(t)G_a^<(t,t) + \sum_k (\dot{V}_{ka}^*(t)G_{ka}^<(t,t) + \mathrm{H.c.})\right], \tag{B5}$$

where $G_a^<(t,t') = \langle c_a^\dagger(t')c_a(t)\rangle$ and $G_{ka}^<(t,t') = \langle c_a^\dagger(t')b(t') c_k(t)\rangle$ with the averages defined in Eq. (B3).

So far, we have calculated the total-energy transfer per unit time into and out of the electronic system. For adsorbates moving slowly along a cyclic trajectory, most of it will be a periodic function of time and will integrate to zero. This is the adiabatic energy transfer of a system maintained in thermal equilibrium at all times during the motion. We are, however, interested in the portion of the energy transfer that results in irreversible energy loss. That contribution has its origin in the nonadiabatic coupling of conduction electrons to the ionic motion, and is referred to as the nonadiabatic energy transfer. We find this contribution by subtracting the adiabatic energy transfer from the total given by Eq. (B5).

In order to calculate the adiabatic energy transfer, we define adiabatic (equilibrium) states $|n_t\rangle$ at time t as solutions of the eigenvalue equation for Hamiltonian $H(t)$ with time treated as a parameter,

$$H(t)|n_t\rangle = E_{n,t}|n_t\rangle. \tag{B6}$$

The energy of a system kept in equilibrium at all times is

$$E_{\mathrm{ad}}(t) = \langle H(t)\rangle_{\mathrm{eq},t} \equiv \mathrm{Tr}\{\rho_{\mathrm{eq}}(t)H(t)\}, \tag{B7}$$

where

$$\rho_{\mathrm{eq}}(t) = e^{\beta\Omega(t)} \sum_n e^{-\beta(E_{n,t} - \mu N)}|n_t\rangle\langle n_t|, \tag{B8}$$

$$e^{-\beta\Omega(t)} = \mathrm{Tr}\, e^{-\beta(H(t) - \mu N)}.$$

Adiabatic processes are characterized by time-independent entropy $S = -\langle \ln\rho_{\mathrm{eq}}(t)\rangle_{\mathrm{eq},t}$. The condition $\dot{S} = 0$ leads to the expression $\dot{E}_{\mathrm{ad}}(t) = \dot{\Omega}(t)$, and the time derivative of $\Omega(t)$ is $\langle \partial H(t)/\partial t\rangle_{\mathrm{eq},t}$. The rate of adiabatic energy transfer thus has the form of Eq. (B5) with the nonequilibrium Green's functions replaced by equilibrium ones [defined in terms of the thermal average (B7) and (B8)].

APPENDIX C: NUMERICAL SOLUTION

In this appendix, we discuss the numerical solution of Eq. (2.12) for open-shell N degenerate adsorbates with $N_0 = 1$ moving at finite but constant speed v. This is done using the equation of motion solution for the nonequilibrium Green's

functions. The first term in Eq. (2.12) contains the adsorbate electron Green's function $G_a^<(t,t')$, which has been calculated by methods described in Shao et al.[26] and Langreth and Nordlander.[27] This section focuses on the calculation of the second term with the off-diagonal Green's function $G_{ka}^<(t,t')$.

The equation of motion for $G_{ka}(t,t')$,

$$\left(i\frac{\partial}{\partial t} - \epsilon_k\right)G_{ka}(t,t') = -i\sum_{a'} V_{ka'}(t)$$
$$\times\langle T_C[c_{a'}(t)b^\dagger(t)b(t')c_a^\dagger(t')]\rangle, \tag{C1}$$

has the formal solution

$$G_{ka}(t,t') = -i\int_C dt'' G_k^0(t,t'')\sum_{a'} V_{ka'}(t'')$$
$$\times\langle T_C[c_{a'}(t'')b^\dagger(t'')b(t')c_a^\dagger(t')]\rangle. \tag{C2}$$

Usual perturbation theory can be applied to the time-ordered product. Within the NCA, the above expression can be written with the aid of the NCA self-energies of the adsorbate level,

$$\Sigma_a(t,t') = i\sum_k V_{ka}^*(t)G_k^0(t,t')V_{ka}(t')B(t,t')$$
$$= iK_a(t,t')B(t,t'). \tag{C3}$$

Due to the separability of the interaction matrix $V_{ka}(t) \equiv u_a(t)v(\epsilon_k)$, the time dependence can be factored out of the k sum in Eq. (2.12):

$$2\mathrm{Re}\sum_k \dot{V}_{ka}^*(t)G_{ka}(t,t) = \frac{\dot{\Delta}(t)}{\Delta(t)}\mathrm{Re}\int_C d\tau\,\Sigma_a(t,\tau)G_a(\tau,t). \tag{C4}$$

The time-ordered equation (C4) can be analytically continued onto the real-time axis and we can write

$$\dot{E}(t) = \sum_a \dot{\epsilon}_a(t)G_a^<(t,t)$$
$$+ \sum_a \frac{\dot{\Delta}(t)}{\Delta(t)}\mathrm{Im}\int_{-\infty}^t d\tau[\Sigma_a^R(t,\tau)G_a^<(\tau,t)$$
$$+ \Sigma_a^<(t,\tau)G^A(\tau,t)], \tag{C5}$$

where $\Sigma_a^{<,R}(t,t') = K_a^<(t,t')B^{<,R}(t,t')$ is the adsorbate electron self-energy. It is expressed in terms of the quantity

$$K_a^<(t,t') = \sum_k V_{ka}^*(t)G_{0,k}^<(t,t')V_{ka}(t')$$
$$= \sqrt{\bar{\Gamma}_a(t)\bar{\Gamma}_a(t')}f^<(t-t'). \tag{C6}$$

Here, $\bar{\Gamma}$ is the band averaged tunneling rate,

$$\bar{\Gamma}_a(t) = \frac{\int d\epsilon\,\Gamma(\epsilon,t)}{\int d\epsilon\,\xi(\epsilon)} = 2\pi|u_a(t)|^2 \tag{C7}$$
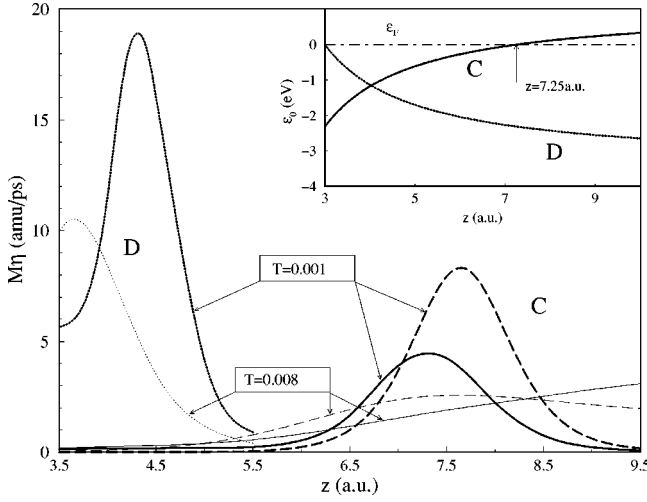
FIG. 8. $M\eta$ in the LFA limit vs the adsorbate-substrate separation z for models D (dotted lines) and C at two temperatures $T = 0.001$ (bold) and 0.008 (thin) Hartree. For model C, we show both the $U=0$, $N=1$ model (dashed lines) and $U=\infty$, $N=2$ model (solid lines).

and

$$f^<(\tau) = \int_{-\infty}^{\infty} \frac{d\epsilon}{2\pi} \xi(\epsilon) f^<(\epsilon) e^{-i\epsilon\tau}, \qquad (C8)$$

where $f^<(\epsilon)$ is the Fermi function, and $\bar{\Gamma}_a(t)$ is related to $\Gamma(\epsilon,t)$ in Eq. (2.10) at the Fermi level through the expression $\Gamma(\epsilon_F,t) = \frac{3}{2}\bar{\Gamma}(t)$.

Equation (C5) then becomes

$$\dot{E}(t) = \sum_a \dot{\epsilon}_a(t) G_a^<(t,t)$$

$$+ \sum_a \frac{\dot{\Delta}(t)}{\Delta(t)} \text{Im} \int_{-\infty}^t dt' [K_a^>(t,t')b(t,t')G_a^{<*}(t,t')$$

$$- K_a^{>*}(t,t')B^{<*}(t,t')g_a^*(t,t')], \qquad (C9)$$

where $g_a(t,t')$ and $b(t,t')$ are defined in Appendix A.

The integrand contains quantities that are all known from the solution of the $G^<(t,t')$ (Ref. 26) and the numerical integration is trivial. The calculation is performed for the nonequilibrium system and the system that is in thermal equilibrium everywhere on its trajectory, and the two contributions are subtracted to yield the nonadiabatic energy transfer.

APPENDIX D: TRADITIONAL MECHANISM FOR FRICTION AND MANY-BODY EFFECTS

This appendix demonstrates the importance of the position dependence of ϵ_0 and Δ for friction in the Kondo region, and discusses the many-body effects in the region $\epsilon_0 \sim \epsilon_F$ where the traditional mechanism produces large frictions.

In Fig. 8, we show the friction $M\eta$ of two models C (solid lines for $U=\infty$ and dashed lines for $U=0$) and D (dotted lines). These models are defined by the image potential form (3.3) along with the same exponentially decaying level width function as before [Eq. (3.2)]. We take the parameters defining the latter to be the same for both models C and D, namely, $\Delta_0 = 1.72$ eV and $b = 0.65$ a.u., while we take $\epsilon_\infty = 1.088$ eV and the minus sign for model C and $\epsilon_\infty = -3.4$ eV and the plus sign for model D. Here we take the empty-orbital region to be above the Fermi level, and the region where the Kondo state can form below, as opposed to the "holelike" description used previously, where the Kondo state could form above. Therefore model D is the analogue of model A in the main text, while model C has the new feature of a Fermi level crossing into the region where the Kondo state can form.

The equilibrium properties of systems C and D are identical at $z = 4.01$ a.u. where the two Newns parameters and their derivatives are the same (see inset of Fig. 8). The Kondo temperature at that point is $T_K = 0.003$ Hartree, but is nearly constant in model C while rapidly decreasing with z in model D. We show in Fig. 8 the friction of the two doubly degenerate systems at temperatures $T = 0.001$ (bold lines) and $T = 0.008$ (thin lines) Hartree. In the interacting model C, there is no visible enhancement over the friction of the equivalent, noninteracting system and $R_K(C) \sim \frac{1}{3}$. On the other hand, the large friction of model D is almost entirely due to the Kondo resonance $[R_K(D) \sim 5]$. Comparison between the Kondo-induced nonadiabaticity at $z = 4.3$ a.u. and that of the traditional mechanisms at $z = 8$ a.u. (where maximum friction of noninteracting model occurs) leads to the rate conditions $[R_K(C)/R_\epsilon] \sim [R_K(C)/R_\Gamma] \sim 0.5$, and implies that many-body enhancements of electronic friction should not be a major factor in model C, as confirmed by our calculations (Fig. 8).

The large frictions of model C near Fermi-level crossing is produced via the conventional mechanism. The width $N\Gamma \sim 0.012$ a.u. at $z = 7.5$ (near the Fermi-level crossing) is small enough to produce large nonadiabatic effects, and make the friction strongly temperature dependent. The adsorbate level crosses ϵ_F at $z = 7.25$ a.u. (see inset of Fig. 8), where we expect the maximum friction of the noninteracting system (dashed lines). However, the two contributions in Eq. (2.15) subtract in the region to the left of the crossing while they add up on the other side. The maximum friction is thus shifted somewhat to the right of the crossing.

The effect of the intra-adsorbate Coulomb repulsion on friction in this regime is twofold. First, the number of single-particle states is not constant in the large U limit, but rather increases with decreasing level occupation (A10). The result is a smaller change in electronic occupation of the adsorbate resonance $\delta n^\infty(t) < \delta n^0(t)$ in Eq. (2.15) as the adsorbate state moves across the Fermi level. This factor reduces the friction in this region. At the same time, however, the effective width Γ_{eff} of the $U=\infty$ Anderson model varies between $N\Gamma$ in the Kondo region and Γ in the empty orbital regime (here at $z \to \infty$). This means that, at large distances, the $N=2$ interacting Anderson model has Γ_{eff} only half the width of the noninteracting system, which in turn enhances its friction over that of the $U=0$ model.

[1] K. P. Bohnen, M. Kiwi, and H. Suhl, Phys. Rev. Lett. **34**, 1512 (1975).

[2] E. G. D'Agliano, P. Kumar, W. Schaich, and H. Suhl, Phys. Rev. B **11**, 2112 (1975).

[3] W. L. Schaich, Surf. Sci. **49**, 221 (1975).

[4] A. Nourtier, J. Phys. (Paris) **38**, 479 (1977).

[5] A. Yoshimori and J. Goto, J. Phys. Soc. Jpn. **44**, 1753 (1978); A. Yoshimori and J. Motchane, *ibid.* **51**, 1826 (1982).

[6] K. Schönhammer and O. Gunnarsson, Z. Phys. B **38**, 127 (1980).

[7] R. Brako and D. M. Newns, J. Phys. C **14**, 3065 (1981).

[8] K. Makoshi, J. Phys. C **16**, 3617 (1983).

[9] B. N. J. Persson and M. Persson, Solid State Commun. **36**, 175 (1980).

[10] R. Ryberg, Phys. Rev. B **32**, 2671 (1985).

[11] C. J. Hirschmugl *et al.*, Phys. Rev. Lett. **65**, 480 (1990).

[12] Ž. Crljen and D. C. Langreth, Phys. Rev. B **35**, 4224 (1987).

[13] A. I. Volokitin and B. N. J. Persson, Phys. Rev. B **52**, 2899 (1995).

[14] T. T. Rantala and A. Rosen, Phys. Rev. B **34**, 837 (1986); M. Head-Gordon and J. C. Tully, J. Chem. Phys. **96**, 3939 (1992).

[15] J. C. Tully, M. Gomez, and M. Head-Gordon, J. Vac. Sci. Technol. A **11**, 1914 (1993).

[16] J. A. Prybyla, T. F. Heinz, J. A. Misewich, M. M. Loy, and J. H. Glownia, Phys. Rev. Lett. **64**, 1537 (1990); J. A. Prybyla, H. W. K. Tom, and G. D. Aumiller, *ibid.* **68**, 503 (1992).

[17] D. M. Newns, T. F. Heinz, and J. A. Misewich, Prog. Theor. Phys. Suppl. **106**, 411 (1991); J. A. Misewich, T. F. Heinz, and D. M. Newns, Phys. Rev. Lett. **68**, 3737 (1992).

[18] M. Brandbyge *et al.*, Phys. Rev. B **52**, 6042 (1995).

[19] D. M. Eigler, C. P. Lutz, and W. E. Rudge, Nature (London) **352**, 600 (1991).

[20] B. C. Stipe *et al.*, Phys. Rev. Lett. **78**, 4410 (1997).

[21] See S. Gao, M. Persson, and B. I. Lundqvist, Phys. Rev. B **55**, 4825 (1997) and references therein.

[22] E. Müller-Hartmann, T. V. Ramakrishnan, and G. Toulouse, Phys. Rev. B **3**, 1102 (1971).

[23] J. W. Gadzuk *et al.*, Surf. Sci. **235**, 317 (1990).

[24] M. Head-Gordon and J. C. Tully, J. Chem. Phys. **103**, 10 137 (1996).

[25] B. Hellsing and M. Persson, Phys. Scr. **29**, 360 (1984); M. Head-Gordon and J. C. Tully, J. Chem. Phys. **96**, 3939 (1992).

[26] H. Shao, D. C. Langreth, and P. Nordlander, Phys. Rev. B **49**, 13 929 (1994).

[27] D. C. Langreth and P. Nordlander, Phys. Rev. B **43**, 2541 (1991).

[28] T. Brunner and D. C. Langreth, Phys. Rev. B **55**, 2578 (1997).

[29] H. Shao, P. Nordlander, and D. C. Langreth, Phys. Rev. Lett. **77**, 948 (1995); Phys. Rev. B **52**, 2988 (1995).

[30] J. W. Rasul and A. C. Hewson, J. Phys. C **17**, 3337 (1984).

[31] A. C. Hewson, *The Kondo Problem to Heavy Fermions* (Cambridge University Press, Cambridge, 1993).

[32] P. Fulde, *Electron Correlations in Molecules and Solids* (Springer, Berlin, 1995).

[33] T. A. Costi, J. Kroha, and P. Wölfle, Phys. Rev. B **53**, 1850 (1996).

[34] P. Coleman, Phys. Rev. B **29**, 3035 (1984).

[35] L. P. Kadanoff and G. Baym, *Quantum Statistical Mechanics* (Benjamin, New York, 1962).

[36] L. V. Keldysh, Zh. Éksp. Teor. Fiz. **47**, 1515 (1964) [Sov. Phys. JETP **20**, 1018 (1965)].

[37] I. Kinoshita, A. Misu, and T. Munakata, J. Chem. Phys. **102**, 2970 (1995).

[38] W. Sesselmann *et al.*, Phys. Rev. Lett. **60**, 1434 (1988).

[39] A. Yoshimori, Surf. Sci. **342**, L1101 (1995).

[40] N. Read, K. Dharamvir, J. W. Rasul, and D. M. Newns, J. Phys. C **19**, 1597 (1986); T. Saso, J. Phys. Soc. Jpn. **58**, 4064 (1989).

[41] D. C. Langreth, Phys. Rev. **150**, 516 (1966).

[42] For scattering particles of unit mass (1 amu) and with $N=2$ (left panel of Fig. 4), the fractional energy loss is 0.29% for $T=0.001$, 0.27% for $T=0.002$, 0.24% for $T=0.004$, and 0.22% for $T=0.008$. The adsorbate is assumed to move at constant speed from infinity to a turning point at $z=2.5$ a.u. where it reverses direction and moves back.